Processing and Application of Ceramics 9 [4] (2015) 203–208
DOI: 10.2298/PAC1504203A

BY-NC-ND

Dielectric studies on cerium doped $BaLa_2Ti_3O_{10}$

Parshuram B. Abhange[1], Vijaykumar C. Malvade[1], Sonnati Chandralingam[2], Shrikant R. Kokare[1,*]

[1]*Department of Physics, Raje Ramrao College, Jath, Dist: Sangli (M.S.) India*
[2]*Jawaharlal Nehru Technological University, Hyderabad, India*

Received 16 November 2015; Received in revised form 10 December 2015; Received in revised form 24 December 2015; Accepted 28 December 2015

Abstract

The $BaLa_{2-x}Ce_xTi_3O_{10}$ samples (with x = 0.2, 0.4, 0.6 and 0.8) were prepared by hydroxide co-precipitation method and finally sintered at 1150 °C. The structure of the prepared samples was characterized by XRD and SEM. The single phase material was confirmed only for the $BaLa_{1.8}Ce_{0.2}Ti_3O_{10}$ ceramics. However, at higher cerium concentration secondary phase was observed. The characteristic plate-like structure, having grains with submicrometer thickness and high aspect ratio, was clearly observed by SEM. The results of dielectric measurement suggest that the appropriate adjustment of doping (with x between 0.2 and 0.8) will give sufficient high dielectric constant at very low loss. The resistivity of samples decreases with increase in temperature indicating the normal semiconducting electrical behaviour.

Keywords: *$BaLa_2Ti_3O_{10}$, structural characterization, electric and dielectric properties*

I. Introduction

Recent discoveries on ferroelectric materials have proved that the perovskite-type ferroelectrics are the most important electronic materials for the technological progress and success. The high permittivity ferroelectric materials have great demand in microwave applications and have been extensively used for piezoelectric transducers, multilayer capacitors, ferroelectric thin film memories etc. [1,2]. Currently, the use of ferroelectric materials for non-volatile, high speed random access memories and dynamic random access memories has also increased [3]. In addition, special attention has been dedicated to environmentally friendly lead-free piezoelectric and ferroelectric materials such as materials with tungsten bronze and leyered-perovskites structures. Thus, materials like $Ba_{2-x}Sr_xNaNb_5O_{15}$ were synthesized for narrow band filters and the high temperature vibration transducer was developed by using the materials like $Bi_4MTi_4O_{15}$ (M = Ca, Sr, Ba) [4]. The increased research interest in lead-free material synthesis and its characterization motivated us to synthesize the proposed system. The high dielectric constant, high quality factor, low dielectric loss and small temperature coefficient of resonant frequency are the most desirable characteristics of the microwave materials [5,6]. It is reported that the compounds present in Ba-Nd-Ti-O system possess excellent temperature stability and dielectric properties [7,8]. The Ba-Nd-Ti-O system is characterized with the mixed compounds like $BaNd_2Ti_3O_{10}$ (BNT), $BaNd_2Ti_4O_{12}$ and $BaNd_2Ti_5O_{14}$ [9]. The reported study on microwave dielectric properties of $BaNd_2Ti_5O_{14}$ shows that it is good for resonator application [10]. It is also reported that the BNT has relatively high dielectric constant, good thermal stability and low loss in the low frequency region [11].

The present paper reports the synthesis and characterization of $BaLa_{2-x}Ce_xTi_3O_{10}$ system with $x = 0.2$, 0.4, 0.6 and 0.8 using hydroxide co-precipitation method.

II. Experimental

2.1. Sample preparation

The $BaLa_{2-x}Ce_xTi_3O_{10}$ powders (with x = 0.2, 0.4, 0.6 and 0.8) were prepared through hydroxide co-precipitation method. The starting raw materials were $Ba(NO_3)_2$, $C_6H_9LaO_6{\times}H_2O$, $Ce(NO_3)_3{\times}6\,H_2O$, $K_2TiO(C_2O_4)_2{\times}2\,H_2O$ and KOH in the form of powders (>99.9% pure). The powders were weighed in stoichiometric proportions and dissolved in distilled wa-

* Corresponding author: tel: +91 9421219424,
fax: +91 2344246251, e-mail: *kshirikant@yahoo.com*

ter separately by constant stirring. These separate solutions were then mixed to form the precipitate at room temperature. The total amount of solution was adjusted to 1000 ml by adding distilled water and heated up to 100 °C for 1 hour by adding liquid ammonia as cleaning agent. After heating, the precipitate was allowed to settle down and the clean water was poured outside. The amount of solution was again adjusted to 1000 ml by adding distilled water and liquid ammonia and heated up to 100 °C for 1 hour by constant stirring. This procedure of cleaning the solution was done three to four times and finally the precipitate was filtered using 0.4 no. filter paper in Buckner Funnel. The filtered material was kept under Infra-Red (IR) lamp for drying. Finally, the dried material was ground for 2 hours in agate mortar by adding acetone.

The ground powders were calcined at 1050 °C for 5 hours. The calcined powders were again ground using acetone for 1 hour and pressed to form the pellets by applying pressure of about 500 MPa. Polyvinyl acetate (PVA) was used as an organic binder for pellet preparation. The prepared pellets were finally sintered in alumina crucible at 1150 °C for 7 hours. After sintering the samples were annealed at the rate of 2 °C/min up to 400 °C and then brought to room temperature by natural rate of cooling.

2.2. Sample characterization

The structural characterization of synthesized samples was made by using X-ray diffraction (XRD) method. The samples were scanned in 2θ range from 20° to 60° with steps of 0.02 using Miniflex-2 Goniometer and CuKα as source of X-rays. The morphological study of the prepared samples was carried out by using scanning electron microscopy (SEM) exposing the samples with 20 kV as an excitation voltage. The hydrostatic weighing method was employed for the density measurement of the prepared samples.

The dielectric properties of the sintered samples were measured using Precessional Impedance Analyzer (Wayne-Kerr 6500B) by varying the temperature from room temperature to 523 K. The laboratory made vertical tubular furnace was used for heating. Using Ohm's law the electrical resistivity of the sintered samples was measured by changing the temperature of the sample and recording the current with nanocurrent meter (Keithly). To adjust the current, the used voltage source was kept constant at 10 volt.

III. Results and discussion

3.1. Structural characterization

Figure 1 illustrates the X-ray diffraction patterns of the sintered $BaLa_{2-x}Ce_xTi_3O_{10}$ samples with various doping amount of cerium. The sintered sample with x = 0.2 showed the typical XRD pattern for the layered-perovskites $BaLa_2Ti_3O_{10}$ ceramics and no additional peaks are observed. The crystal structure and lattice parameters are in good agreement with the reported data [12,13] and the indexed XRD peaks with the corresponding *hkl* lines (PCPDF file no. 430253), that additionally confirmed the single phase material. Incorporation of cerium in $BaLa_2Ti_3O_{10}$ structure on lanthanum site can be expected due to the compatible size of their ionic radii (for lanthanum 1.061 Å and cerium 1.034 Å). However, with the higher amount of cerium substituting lanthanum additional XRD peaks can be seen. Thus, the intensity of the XRD peak at around 29° becomes much higher with the Ce addition. It can be an indication of the secondary phase, which could be pyrohlore phase.

The surface morphology of the prepared materials was studied by using scanning electron microscopy (Fig. 2). The characteristic plate-like structure, having grains with submicrometer thickness and high aspect ratio, can be clearly observed. The observed grain size is far less than the earlier reported for ceramics in BaO-Nd_2O_3-TiO_2 system [10]. In addition, even though the density of the material is about 98% TD measured by hydrostatic weighing method, SEM images confirm the presence of open porosity.

3.2. Dielectric properties

Figure 3 shows the relative permittivity of the sintered $BaLa_{2-x}Ce_xTi_3O_{10}$ ceramics versus temperature for different frequencies. It can be seen that at 1 MHz dielectric constant of $BaLa_{1.8}Ce_{0.2}Ti_3O_{10}$ ceramics is about 40 and above the temperature of 450 K slightly

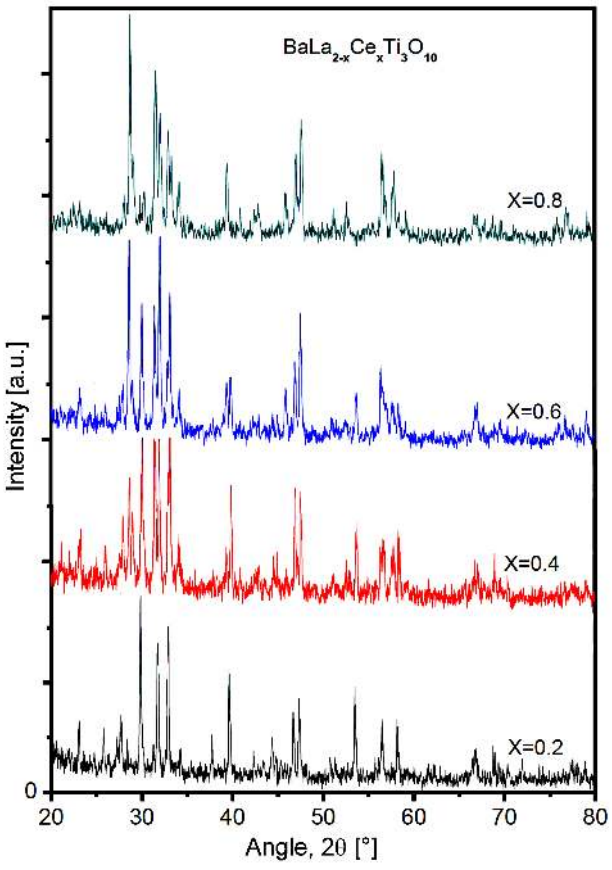

Figure 1. XRD patterns of $BaLa_{2-x}Ce_xTi_3O_{10}$

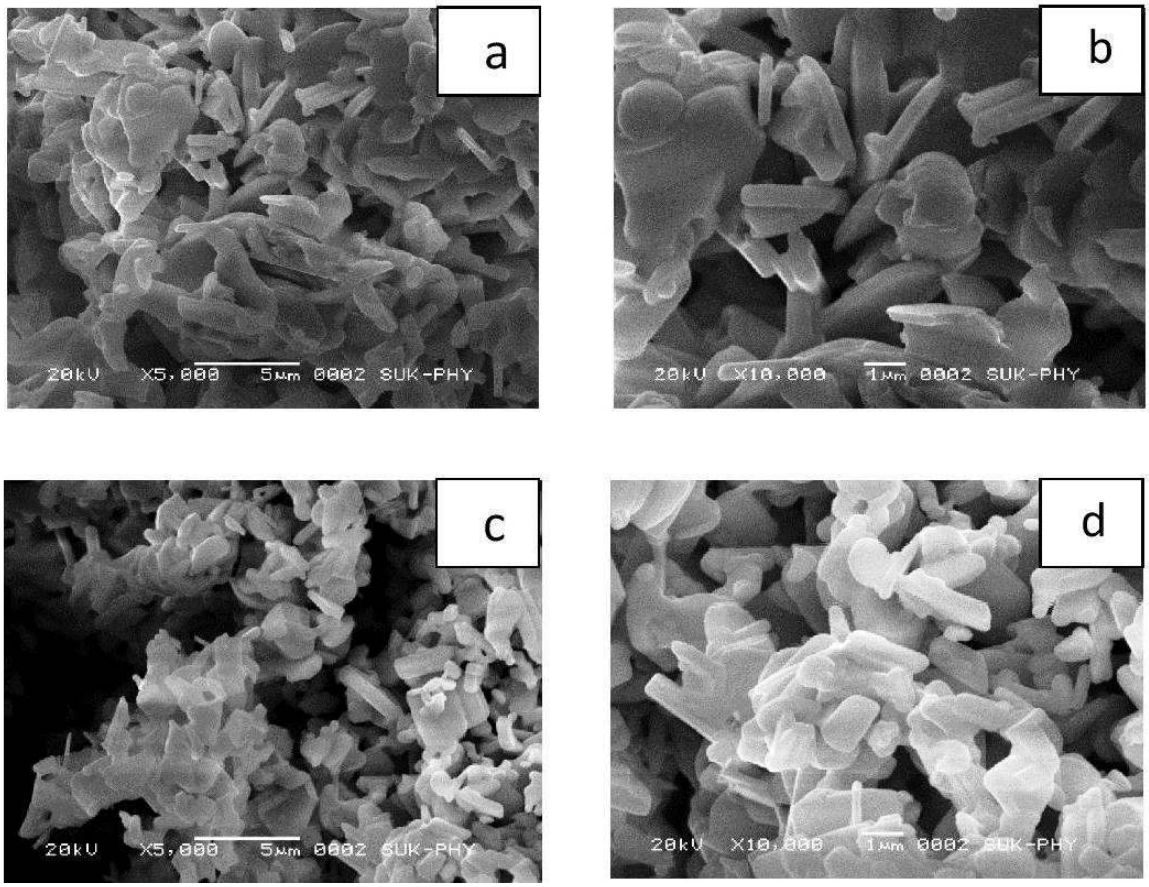

Figure 2. SEM micrographs of (a, b) $BaLa_{1.8}Ce_{0.2}Ti_3O_{10}$ and (c, d) $BaLa_{1.6}Ce_{0.4}Ti_3O_{10}$

increases. The increase of dielectric constant is also observed with the decrease of frequency (Fig. 3). Similar behaviour that the dielectric constant does not significantly depend on the temperature variation was reported for barium neodymium titanate ceramics [14]. From Fig. 3 and Table 1 it can also be observed that the dielectric constant of the samples increases with increase in the doping concentration of cerium to $x = 0.6$. In the prepared ceramics, La^{+3} is being replaced by Ce^{+4} which gives more donor carriers and this could be the reason for the increase of dielectric constant. However, dielectric properties can also be influenced by the characteristic nature of Ce which can change its oxidation states easily between +3 and +4 and, thus, has different role in creation of structural defects. On the other hand, it is observed that for the sample $BaLa_{1.2}Ce_{0.8}Ti_3O_{10}$ with $x = 0.8$ the dielectric constant decreases (Fig. 3). The observed changes at higher cerium concentration can be related to the presence of the secondary phase.

Figure 4 shows the dielectric loss of the sintered $BaLa_{2-x}Ce_xTi_3O_{10}$ ceramics versus temperature for different frequencies. It is obvious that the sample with lower amount of cerium ($x = 0.2$) has relatively low dielectric loss and with the increase of cerium content an increase of $\tan\delta$ is evident (Fig. 4). The reason could be existence of the secondary phase.

Such types of materials can be useful in microwave devices which have sufficient dielectric constant at very low loss. This is an indicative characteristic of the materials which can be used for microwave devices.

3.3. Electron transport properties

The variations of electrical resistivity with temperature and activation energy with cerium doping concentration are presented in Figs. 5 and 6, respectively. The resistivity of samples decreases with increase in temperature indicating on the normal semiconducting electrical behaviour. The $\ln(\rho)$ *vs.* $1000/T$ graph shows a linear decrease of the $\ln(\rho)$ with increasing the temperature for all samples. The decrease in resistivity with tempera-

Table 1. The variation of relative permittivity and loss factor for different concentrations at room temperature at 1 kHz

Samples	x	ε_r	$\tan\delta$
$BaLa_2Ti_3O_{10}$	0.00	<100 [ref. 12]	1.2 [ref. 12]
$BaLa_{1.8}Ce_{0.2}Ti_3O_{10}$	0.2	47	0.096
$BaLa_{1.6}Ce_{0.4}Ti_3O_{10}$	0.4	61	0.18
$BaLa_{1.4}Ce_{0.6}Ti_3O_{10}$	0.6	122	0.46
$BaLa_{1.2}Ce_{0.8}Ti_3O_{10}$	0.8	80	0.44

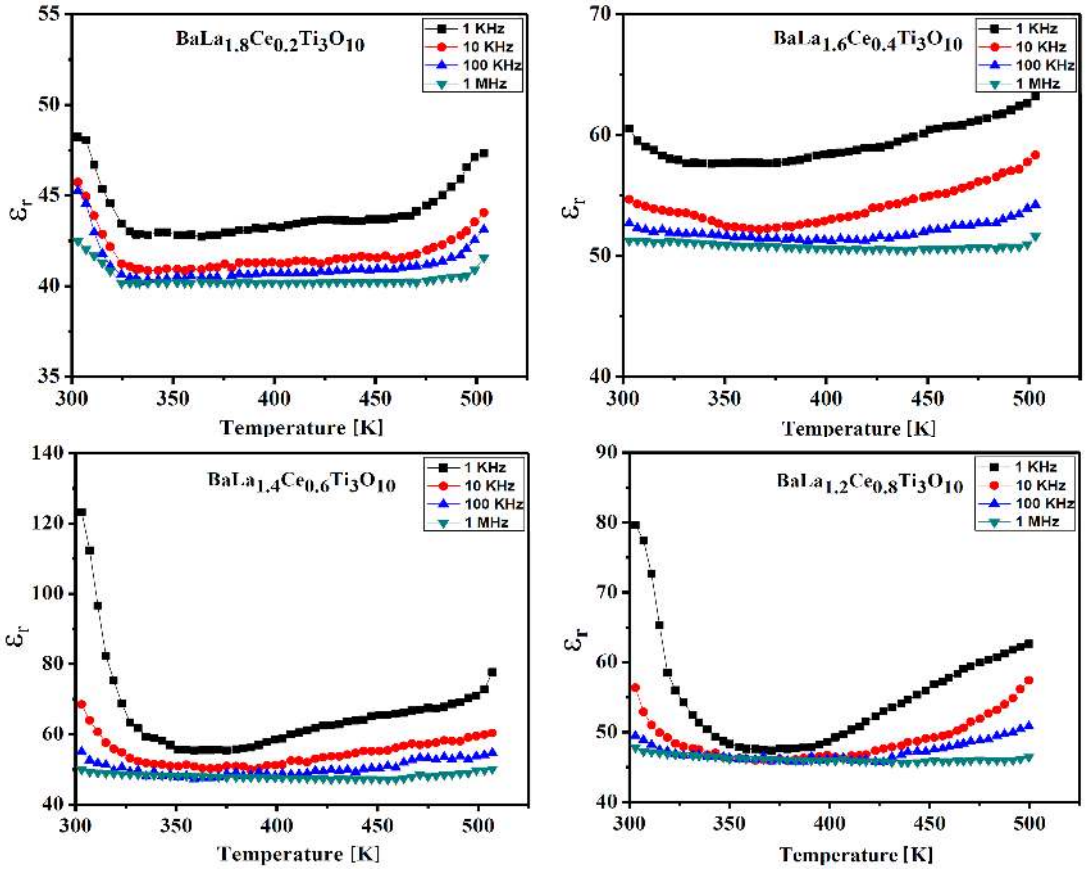

Figure 3. Dielectric constant versus temperature for $BaLa_{2-x}Ce_xTi_3O_{10}$ ceramics (x = 0.2, 0.4, 0.6 and 0.8)

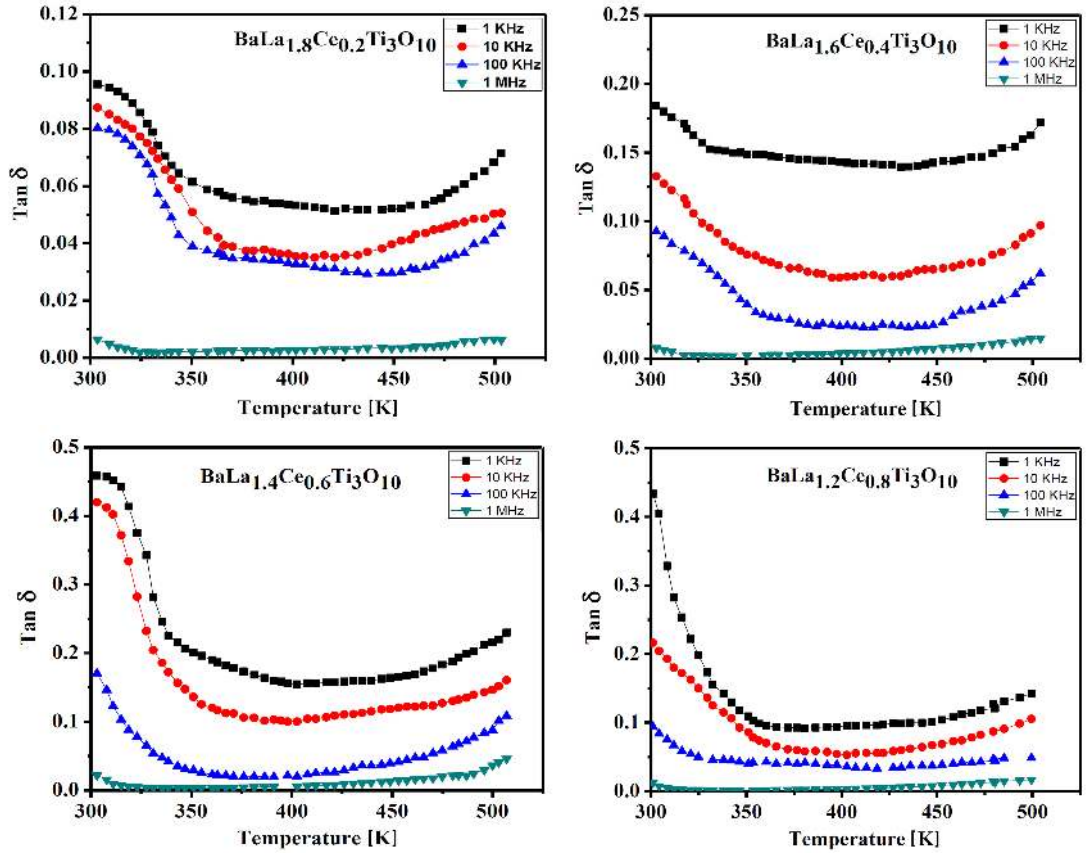

Figure 4. Loss factor versus temperature for $BaLa_{2-x}Ce_xTi_3O_{10}$ ceramics (x = 0.2, 0.4, 0.6 and 0.8)

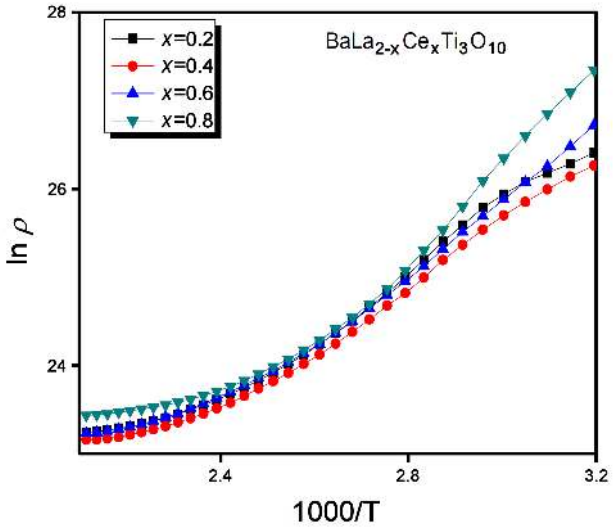

Figure 5. Temperature dependence of electrical resistivity

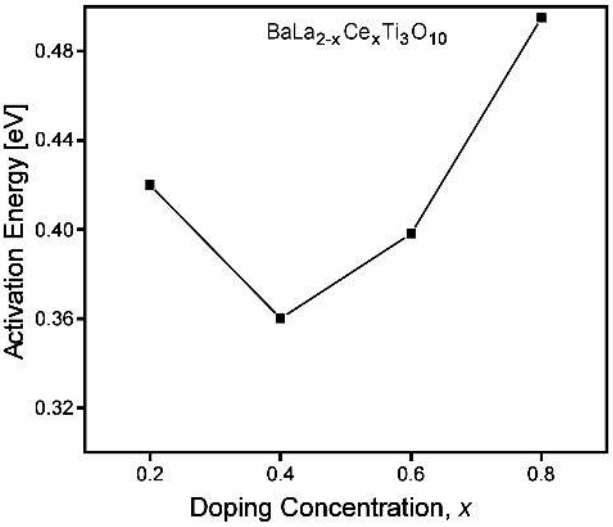

Figure 6. Variation of activation with doping concentration

ture is principally due to the thermally induced mobility of the charge carriers (electrons or holes) rather than to thermally generated charge carriers [15]. The value of the activation energy was found to be less than 0.5 eV and is in good agreement with the trends observed in the plots of temperature dependent dielectric constant values. However, it is clearly seen that the resistivity has two distinct conduction mechanisms. The change from a straight line region through a low gradient to one with an elevated gradient as temperature is increased implies that extra conduction mechanisms are involved. The decrease of electrical resistivity at higher temperature was due to the increase in drift mobility of the charge carriers [16]. The exponential law can express the temperature dependence of the electrical resistivity:

$$\rho = \rho_0 \exp\left(\frac{E_a}{k \cdot T}\right) \quad (1)$$

where, ρ is the resistivity at temperature T, ρ_0 is a parameter depending on the sample characteristics (structure, thickness, etc.) and is constant, E_a denotes the thermal activation energy of electrical conduction, and T is the absolute temperature and k the Boltzmann's constant [17].

IV. Conclusions

The cerium doped $BaLa_2Ti_3O_{10}$ materials were obtained by hydroxide co-precipitation, pressing and sintering at 1150 °C. XRD confirmed the single phase material only for the $BaLa_{1.8}Ce_{0.2}Ti_3O_{10}$ ceramics. However, at higher cerium concentration secondary phase was observed. The characteristic plate-like structure, having grains with submicrometer thickness and high aspect ratio, was clearly observed by SEM. The increased dielectric constant for higher doping level with small dielectric loss is indication that material can be useful for microwave dielectric resonators. However, to get any final conclusion one may need to study the dielectric response at microwave frequencies. The activation energy trend is also suggesting that fine tuning of substitution is needed.

References

1. T. Ramoska, J. Banys, R. Sobiestianskas, M.V. Petrovic, J. Bobic, B. Stojanovic, "Dieectric investigations of La-doped barium titanate", *Process. Appl. Ceram.*, **4** [3] (2010) 193–198.
2. F. Wan, J.G. Han, Z.Y. Zhu, "Dielectric response in ferroelectric $BaTiO_3$", *Phys. Lett. A*, **372** (2008) 2137–2140.
3. M.P. McNeal, S.J. Jang, R.E. Newnham, "The effect of grain and particle size on the microwave properties of barium titanate ($BaTiO_3$)", *J. Appl. Phys.*, **83** [6] (1998) 3288–3297.
4. Y.-Q. Lu, Y.-X. Li, "A review on lead-free piezoelectric ceramics studied in china", *J. Adv. Dielectrics*, **1** [3] (2011) 269–288.
5. D. Kajfez, P. Guillon, *Dielectric Resonators*, Artech House, Norwood, MA, 1986.
6. E.A. Nenasheva, N.F. Kartenko, "High dielectric constant microwave ceramics", *J. Eur. Ceram. Soc.*, **21** (2001) 2697–2701.
7. H. Ohsato, S. Nishigaki, T. Okuda, "Superlattice and dielectric proparties of BaO-R_2O_3-TiO_2 (R=La, Nd and Sm) microwave dielectric compounds", *Jpn. J. Appl. Phys.*, **31** (1992) 3136–3138.
8. J.H. Choi, J.H. Kim, B.T. Lee, Y.M. Kim, J.H. Moon, "Microwave dielectric properties of Ba-Nd-Ti-O system doped with metal oxide", *Mater. Lett.*, **44** [1] (2000) 29–34.
9. A. Yamada. Y. Utsumi, H. Watarai, "The effect of Mn addition on dielectric properties and microstructure of BaO-Nd_2O_3-TiO_2 ceramics", *Jpn. J. Appl. Phys.*, **30** (1991) 2350–2353.
10. R. Ratheesh, H. Sreemoolanadhan, M.T. Sebastian, P. Mohanan, "Preparation, characterization and di-

electric properties of ceramics in the BaO-Nd_2O_3-TiO_2 system", *Ferroelectrics*, **211** (1998) 1–8.
11. D. Kolar, S. Gaberscek, B. Volavsek, H.S. Parker, R.S. Roth, "Synthesis and crystal chemistry of $BaNd_2Ti_3O_{10}$, $BaNd_2Ti_5O_{14}$, and $Nd_4Ti_9O_{24}$", *J. Solid State Chem.*, **38** [2] (1981) 158–164.
12. M.M. Sutar, "Structural and dielectric properties of modified barium titanate ($BaTiO_3$) for microwave applications", *M. Phil. Thesis*, Madurai Kamraj University, Madurai, India, 2008.
13. S.K. Singh, V.R.K. Murthy, "Crystal structure, Raman spectroscopy and microwave dielectric properties of layered-perovskite $BaA_2Ti_3O_{10}$ (A = La, Nd and Sm) compounds", *Mater. Chem. Phys.*, **160** (2015) 187–193.
14. C.H. Lu, Y.H. Haung, "Densification and dielectric properties of barium neodymium titanium oxide ceramics", *Mater. Sci. Eng. B*, **98** (2003) 33–37.
15. N. Iftimie, E. Rezlescu, P.D. Popa, N. Rezlescu, "Gas sensitivity of nanocrystalline nickel ferrite", *J. Optoelectron. Adv. Mater.*, **8** (2006) 1016–1018.
16. R.S. Devan, Y.D. Kolekar, B.K. Chougule, "Effect of cobalt substitution on the properties of nickel-copper ferrite", *J. Phys.: Condens. Matter*, **18** (2006) 9809–9821.
17. D.S. Dhawale A.M. More, S.S. Latthe, K.Y. Rajpure, C..D. Lokhande, "Room temperature synthesis and characterization of CdO nanowires by chemical bath deposition (CBD) method", *Appl. Surface Sci.*, **254** (2008) 3269–3273.